Journal of Polymer Research (2021) 28: 101
https://doi.org/10.1007/s10965-020-02404-x

ORIGINAL PAPER

Synthesis and properties of strong and tough Diels–Alder self-healing crosslinked polyamides

Jinnan Zhao[1] · Shuo Chen[1] · Jingbo Zhao[1] · Zhiyuan Zhang[1] · Junying Zhang[1]

Received: 25 August 2020 / Accepted: 28 December 2020 / Published online: 2 March 2021

Abstract

A new method was provided to synthesize Diels–Alder (DA) self-healing cross-linked polyamides (SH-cPAs) with high tensile strength and good self-healing efficiency. A furfurylamine-N,N'-bis(methyl propionate) (FA-BMP) was synthesized through the Michael addition of furfurylamine and methyl acrylate. Bulk polycondensation of FA-BMP with bis(2-aminopropyl) polypropylene glycol and *m*-xylylenediamine were conducted, and several polyamide prepolymers containing furan pendent groups (pFU-PAs) were synthesized. From a DA reaction between pFU-PAs and 1,5-bismaleimido-2-methylpentane, different SH-cPAs were prepared. The pFU-PAs were characterized by ^{1}H NMR, ^{13}C NMR, FT-IR, amine values, and size exclusion chromatography. The DA reaction in SH-cPAs were demonstrated by FT-IR and ^{1}H NMR spectra. Their thermally repairing was verified with polarizing optical microscopy and tensile tests. SH-cPAs exhibits tensile strength up to 37 MPa with strain at break of 27%-164%. Their tensile strength after self-repairing was still up to 26 MPa with self-healing efficiency of 70%-92%.

Keywords Cross-linked polyamides · Self-healing polymers · Michael addition · Polycondensation · Diels–alder reaction

Introduction

Cross-linked polymers including cross-linked polyamides, polyurethanes, epoxy resins, and acrylic resins exhibit excellent dimension stability, mechanical properties, and organic solvent resistance. They are used widely as adhesives [1], coatings [2], and composite matrix. In the process of handling, transportation, storage, and applications, defect, internal stress, and external force often cause micro or macro damages inside, and eventually worsen mechanical properties and reduce service life [3, 4]. However, popular cross-linked polymers lack re-fabrication ability and are difficult to be repaired. Recently, scientists have developed many self-healing (SH) methods to cross-linked polymers [5].

SH crosslinked polymers are generally divided into extrinsic aid [6, 7] and intrinsic aid types [8]. Intrinsic types are synthesized usually through reversible dynamic covalents or non-covalent structures. The reversible non-covalent structures used include hydrogen bond self-repair [9], metal ligand self-repair [10], and ionic self-repair [11]; while the reversible covalent structures include reversible C = N bonds [12], disulfide bonds [13], C-ON bonds [14], and Diels–Alder (DA) reaction [15–17]. Among them, DA reaction is particularly ideal for preparing thermally stimulated SH polymers due to its excellent thermal reversibility, good yield, mild reaction condition, and few side reactions. Most studies of DA SH polymers are fixed on the maleimide (dienophile) and furan (diene) systems, in which maleimide groups show sufficiently high reactivity [18–21]. Up to now, DA reaction has been widely applied in SH epoxy resins [17, 19, 22] and polyurethanes [15, 20], but is still rarely used in SH cross-linked polyamides (SH-cPAs). Liu et al. had synthesized DA SH-cPA gels from a tri-functional furan compound and aromatic PAs containing maleimide pendent groups [23].

✉ Jingbo Zhao
zhaojb@mail.buct.edu.cn

✉ Junying Zhang
zhangjy@mail.buct.edu.cn

[1] Key Laboratory of Carbon Fiber and Functional Polymers (Beijing University of Chemical Technology), Ministry of Education; College of Materials Science and Engineering, Beijing University of Chemical Technology, Beijing 100029, China

Scheme 1 Synthesis of FA-BMP and FA-MP

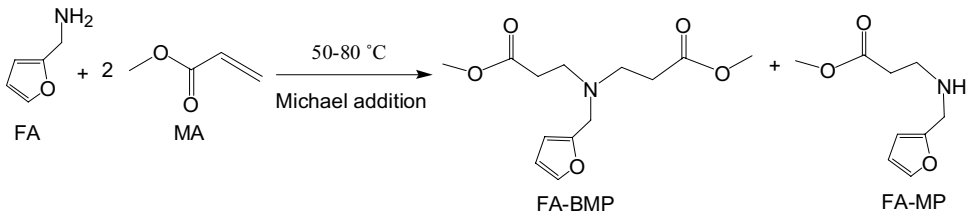

In this study, a furfurylamine-N,N-bis(methyl propionate) (FA-BMP) was synthesized first via a Michael addition between methyl acrylate (MA) and furfurylamine (FA). Bulk polycondensation of FA-BMP with bis(2-aminopropyl) polypropylene glycol (D230) and *m*-xylylenediamine (MXDA) were conducted, and three linear polyamide prepolymers containing furan pendent groups (pFU-PAs) were prepared. Then, SH-cPAs were prepared from the DA reaction between pFU-PAs and 1,5-bismaleimido-2-methylpentane (BMIMP). These SH-cPAs show excellent mechanical properties and good self-healing properties.

Experimental

Materials

MA (99%) and MXDA (99%) were purchased from Aladdin in Shanghai, China. FA (99%) was bought from Alfa Aesar Co. Ltd. D230 was purchased from Beijing Hua Wei Rui Ke Co. BMIMP was prepared according to the reference [24]. The yield of BMIMP was 74%, and the melting point was 89 °C. Its structure was confirmed by ^{1}H NMR (Fig. S1) and ^{13}C NMR (Fig. S2) spectra.

Synthesis of FA-BMP

In a 100 mL three-necked flask, 14.6 g (0.15 mol) FA and 25.8 g (0.30 mol) MA were stirred mechanically at 50 °C for 3 h under normal pressure to conduct bulk Michael addition. In order to react fully, the reaction was maintained at 80 °C for 2 h, and a pale yellow liquid FA-BMP was obtained with the yield of 95% (Scheme 1).

Synthesis of pFU-PAs

pFU-PAs were demonstrated as pPA-FU-*x*%s, in which *x*% was the molar percent of MXDA (0 mol%, 10 mol%, and 20 mol%) in diamines (D230 and MXDA). In different 50 mL three-necked flasks, Fu-BMP, D230 and MXDA were added at 6:5 ester:H_2N- or Fu-BMP/(D230 + MXDA) molar ratio and at 0 mol%, 10 mol%,

Scheme 2 Synthesis of pFU-PA-*x*%s

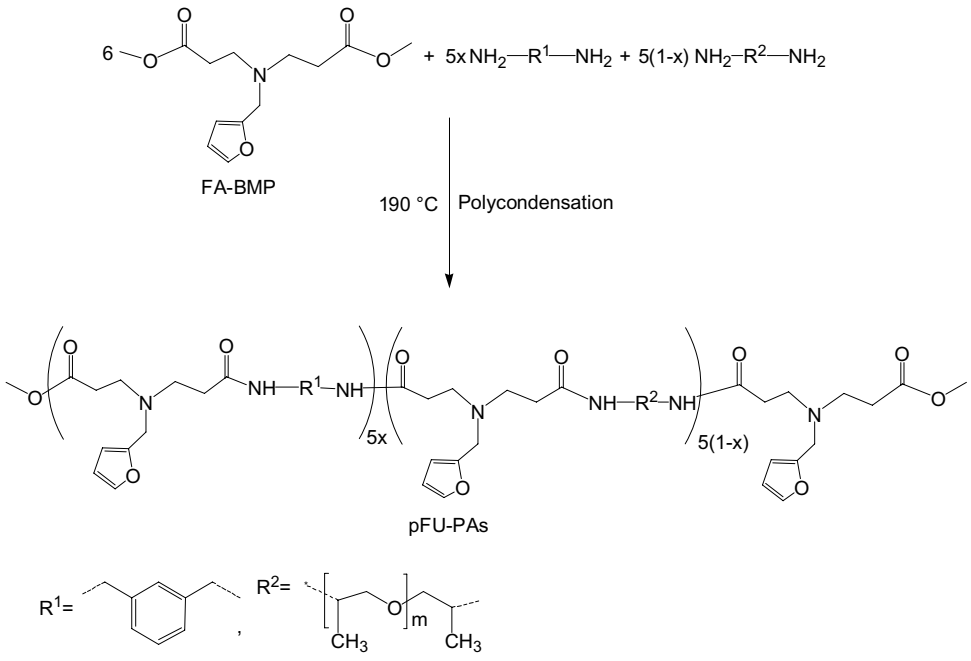

Scheme 3 Synthesis of SH-cPAs

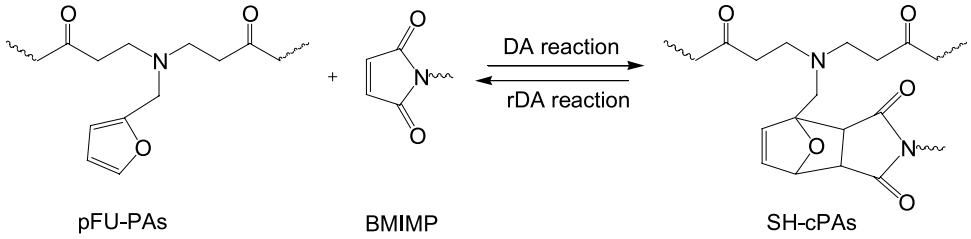

or 20 mol% MXDA in total diamines. The mixtures were stirred mechanically at 190 °C for 10 h under N_2, and then for 1 h under the reduced pressure of 3990 Pa to remove the formed methanol and unreacted reactants. Three light brown pFU-PAs, i.e. pFU-PA-0%, pFU-PA-10%, and pFU-PA-20%, were obtained (Scheme 2). Their yield was approximately 85%.

Synthesis of SH-cPAs

The SH-cPAs were demonstrated as SH-cPA-*x*%s, in which *x*% was the MXDA molar percent (0 mol%, 10 mol%, or 20 mol%) in diamines used in the preparation of pFU-PAs. In three 10 mL beakers, pFU-PAs and BMIMP were added at the 1:1 molar ratio between the furan rings in pFU-PAs and the maleimide groups in BMIMP (Fu/MI). The mixtures were stirred to uniformity at 130 °C, and were transferred into dumbbell tetrafluoroethylene molds. Bubbles formed during mixing were removed at 130 °C under a reduced pressure of 3990 Pa. Then, the samples were cured in a vacuum oven at 60 °C for 30 h to obtain dumbbell SH-cPA-0%, SH-cPA-10%, SH-cPA-20% films (Scheme 3).

Characterization

The amine value was detected according to the procedure described in literature [25]. The M_n, M_w, and dispersity (D) of pFU-PAs were characterized on Waters 150C size exclusion chromatography (SEC) at 25 °C with tetrahydrofuran as eluent (1 mL/min) and polystyrene as standards. Fourier transform infrared (FT-IR) spectroscopy was performed on a NICOLET60SXB spectrometer in the range from 4000 to 400 cm^{-1}. ^1H and ^{13}C NMR spectroscopy was performed on an Avance-400 spectrometer (Brook, Switzerland) with hexadeuterium dimethylsulfoxide (DMSO-*d*6) as the solvent. Differential scanning calorimetry (DSC) was performed on TA Instruments Q2000. The samples were first cooled to -50 °C, and then heated to 200 °C at a rate of 10 °C/min under nitrogen atmosphere.

The dissolution ratio of SH-cPAs was detected by soaking them in DMF at 60 °C for 8 h. The left parts were filtrated, washed with ethanol, and dried in vacuum oven at 60 °C to constant weight. The dissolution ratio was calculated according to Eq. (1).

$$\text{Dissolution ratio (\%)} = \frac{\text{Initial weight - final weight}}{\text{Initial weight}} \times 100\% \quad (1)$$

The repairing of the cracks on SH-cPA surface was observed at 130 °C on a dm2500p polarizing optical microscope (POM). The mechanical properties of SH-cPAs were recorded on a LLOYD LR30K tensile testing machine at a tensile speed of 5 mm/min. Dumbbell samples (10 × 4 × 1 mm) were used in the tensile test. Original dumbbell splines were cut from middle and put together in dumbbell-shaped molds. They were heated at 130 °C for 2 h and then placed in an oven at 60 °C for 30 h. The self-healing efficiency was calculated according to Eq. (2):

$$\text{Self - healing efficiency (\%)} = \frac{\text{Self - healed tensile strength}}{\text{Original tensile strength}} \times 100\% \quad (2)$$

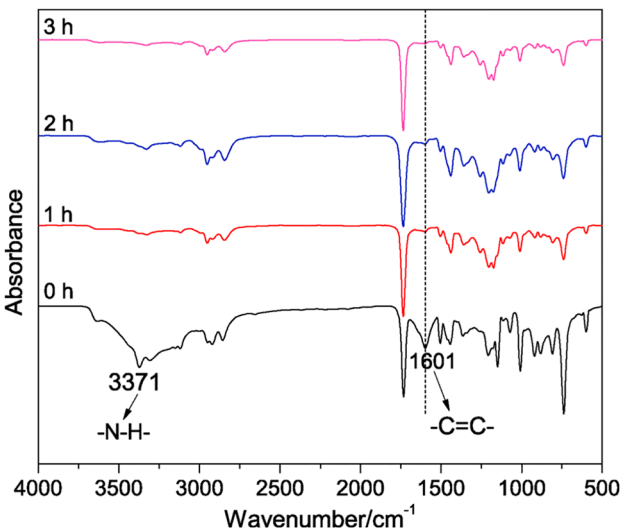

Fig. 1 Monitoring FT-IR spectra in the preparation of FA-BMP

Results and discussion

FA-BMP synthesis

FA-BMP was prepared from the Michael addition of FA and MA at a 1:2 FA/MA molar ratio. The reaction was monitored by FT-IR spectra (Fig. 1). At 0 h, the νC=C peak of MA emerged at 1601 cm^{-1}, while the νN-H peak of FA appeared at 3371 cm^{-1}. They decreased with the time increasing. At 3 h, these two peaks became negligible. In order to make FA and MA react fully, the reaction was continued for 2 h at 80 °C under nitrogen.

The obtained FA-BMP was characterized by ^{1}H NMR spectrum (Fig. 2). It contained some unreacted MA. Meanwhile, some furfurylamine-N-methyl propionate (FA-MP) was also contained. The conversion of MA was calculated according to Eq. (3), and was around 67%. Scheme 1 shows the formation of FA-BMP and FA-MP. Due to low reactivity of the –NH- group in FA-MP, MA was not reacted completely, and some FA-MP was left.

$$\text{MA conversion}(\%) = \frac{\frac{A^0_{10'}}{A^0_5} - \frac{A_{10'}}{A_5}}{\frac{A^0_{10'}}{A^0_5}} \times 100\% \quad (3)$$

In which $A_{10'}{}^0$ and $A_5{}^0$ were the initial peak areas of 10′ and 5 protons, while $A_{10'}$ and A_5 were their areas at t moment.

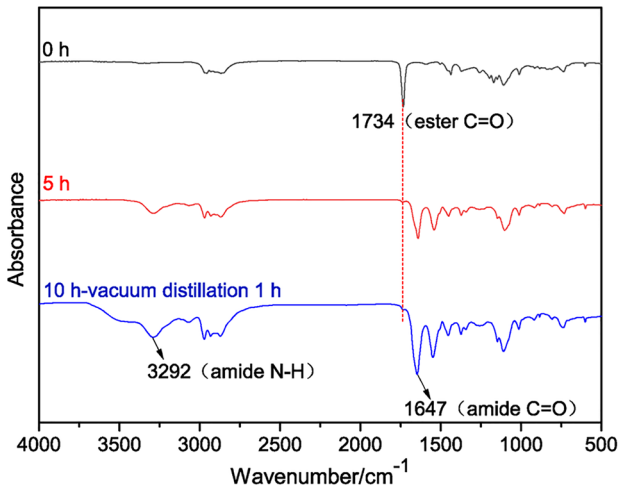

Fig. 3 FT-IR spectrums of pFU-PA-10% at different time

pFU-PA-x% synthesis

Bulk polycondensation of FA-BMP with D230 and MXDA was conducted at an ester:H_2N- molar ratio of 6:5 and different MXDA molar percentages in diamines, and three linear pFU-PAs were prepared (Scheme 2).

The bulk polymerization of pFU-PA-10% was monitored with FT-TR spectra (Fig. 3). The ester νC=O peak (1734 cm^{-1}) of original FA-BMP decreased with the increase of reaction time, while the amide νC=O (1647 cm^{-1}) and νN-H (3292 cm^{-1}) peaks of the forming pFU-PA-10% increased. After normal pressure (10 h) and

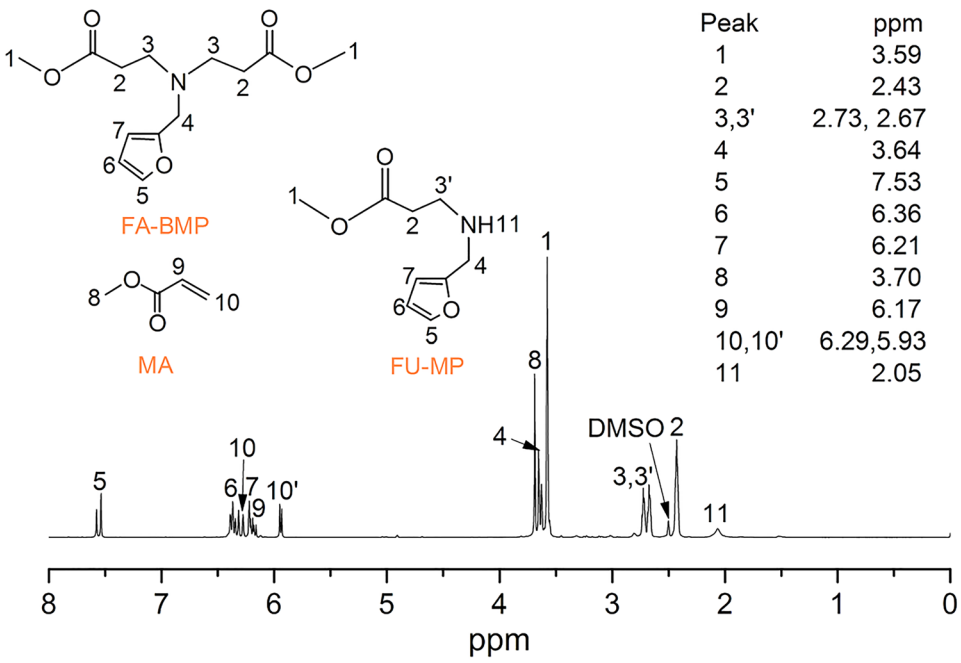

Fig. 2 ^{1}H NMR spectrum (*d*6-DMSO) of FA-BMP

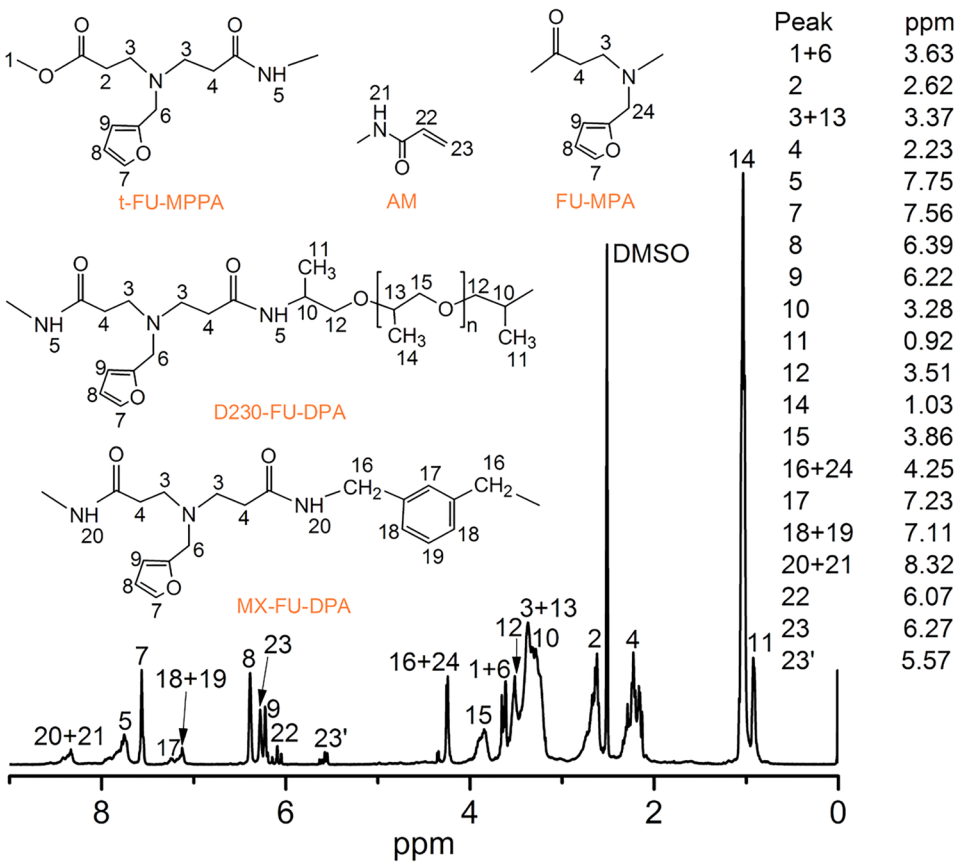

Fig. 4 ^{1}H NMR spectrum (*d*6-DMSO) of pFU-PA-10%

reduced pressure (1 h) reaction, the ester *v*C = O peak became a tiny weak peak, which was related to the ester terminal groups of pFU-PA-10%. Polycondensation of FA-BMP, D230 and MXDA was nearly complete at 11 h.

The structure of pFU-PA-10% was confirmed by ^{1}H-NMR spectrum (Fig. 4), in which the protons were designated based on the references [26, 27]. pFU-PA-10% was composed of the terminal furfurylamine-N-(methyl propionate)-N-propionamide (t-FU-MPPA) segments, D230 furfurylamine-N,N-dipropionamide (D230-FU-DPA) segments, *m*-xylylene furfurylamine-N,N-dipropionamide (MX-FU-DPA) segments, acrylamide (AM) segments, and furfurylamine-N-mono propionamide (FU-MPA) segments. pFU-PA-10% was terminated with ester groups. The D230-FU-DPA and MX-FU-DPA segments were formed from the reaction of FA-BMP with D230 and MXDA, respectively. The amide peaks of the D230-FU-DPA and MX-FU-DPA segments were found at 7.75 and 8.32 ppm. pFU-PAs with many middle amide groups and ester terminal groups were prepared. As FA-BMP contained some unreacted MA, MA reacted with the H_2N- groups of D230 or MXDA at high temperature and resulted in the AM segments. The extra peaks found at 5.57, 6.07, and 6.27 ppm belonged to the 23′, 22, and 23 protons of AM. The peak at 4.25 ppm contained the 24 –CH_2– protons of FA-MPA segments, which were formed from the self-polycondensation of FA-MP. Figure S3 shows the ^{13}C NMR spectrum (*d*6-DMSO) of pFU-PA-10%, and Fig. S4 exhibits the structure units related to the ^{13}C NMR spectrum. The structure of pFU-PA-10% was also confirmed by ^{13}C NMR characterization.

The initial and final amine values of pFU-PA-x%s were determined. The reaction extent of polymerization

Table 1 Amine values and SEC data of pFU-PA-x%

pFU-PA-x%	D230:MXDA (Molar ratio)	Amine value [a] (mgKOH·g^{-1})		Reaction extent [b] (%)	M_n (SEC)	M_w (SEC)	D (SEC)
		Initial	Final				
pFU-PA-0%	100:0	229.37	28.31	87.66	1190	1350	1.13
pFU-PA-10%	90:10	233.85	40.81	82.55	1200	1360	1.13
pFU-PA-20%	80:20	238.52	45.52	80.92	1220	1390	1.14

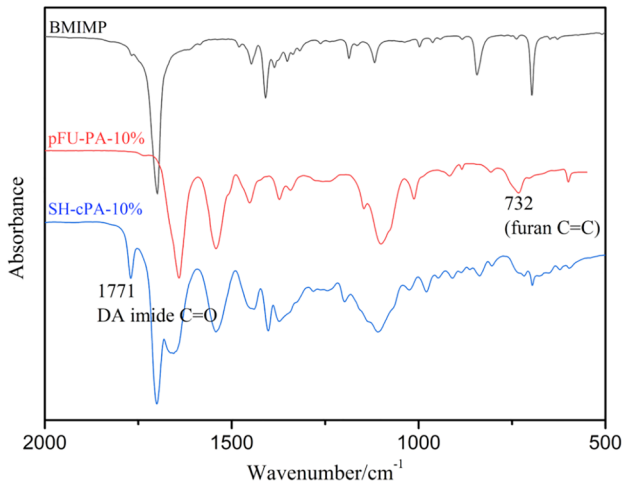

Fig. 5 FT-IR spectra of BMIMP, pFU-PA-10%, and SH-cPA-10%

calculated from amine values was in the range from 80.92% to 87.66%. SEC characterization showed that the M_n of pFU-PA-x%s ranged from 1194 to 1221 g/mol. Low molecular weight pFU-PA-x%s were prepared (Table 1).

[a] The amine value was calculated using: Amine value $= \frac{56.1c(V_0-V_s)}{m}$, in which V_0 and V_s (mL) were the consumed volume of KOH solution in the blank assay and sample; whereas 56.1, c (mol/L), and m (g) were the molecular weight (g/mol) of KOH, the concentration of KOH solution, and the weight of sample, respectively.

[b] The reaction extent was calculated according to:

$$\text{Reaction extent (\%)} = \frac{\text{Initial amine value - Final amine value}}{\text{Initial amine value}} \times 100\%$$

SH-cPA synthesis

SH-cPAs were prepared from the reaction of pFU-PAs and BMIMP at a 1:1 Fu/MI molar ratio (Scheme 3).

Figure 5 shows the FT-IR spectra of BMIMP, pFU-PA-10%, and SH-cPA-10%. Compared to pFU-PA-10% and BMIMP, SH-cPA-10% shows a clear absorption peak at 1771 cm^{-1}, which corresponds to the imide $\nu C=O$ peak of the newly generated DA adduct. At the same time, the absorption peak of the furan rings (732 cm^{-1}) in SH-cPA-10% was weakened. They all prove the occurrence of DA reaction. Different from the ^1H NMR spectrum of pFU-PA-10% (Fig. 6), SH-cPA-10% exhibits the characteristic peaks of the DA adducts at 2.96, 3.05, 5.08 and 6.52 ppm which correspond to the 15, 16, 14, and 13 hydrogens in SH-cPA-10%. Figures S5 and S7 show the ^1H and ^{13}C NMR spectra of SH-cPA-10% in detail. Figures S6 and S8 show the structure unis related to its ^1H NMR and ^{13}C NMR spectra. The ^1H and ^{13}C NMR results are consistent with those of FT-IR characterization,

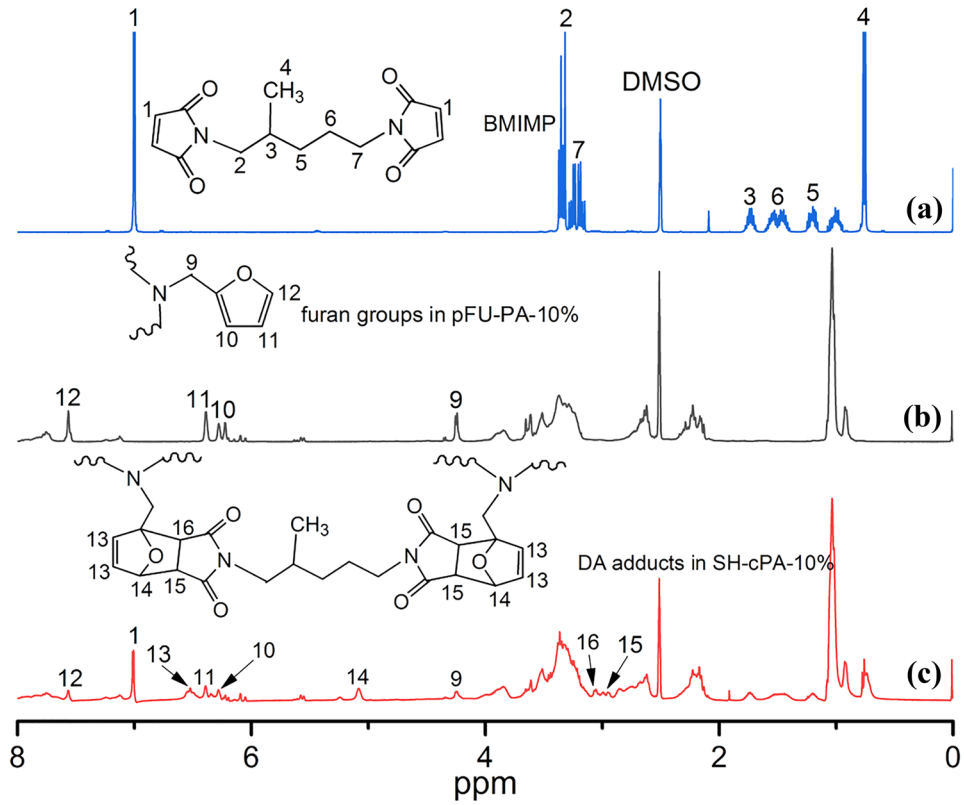

Fig. 6 ^1H NMR spectra (*d*6-DMSO) of BMIMP (**a**), pFU-PA-10% (**b**), and SH-cPA-10% (**c**)

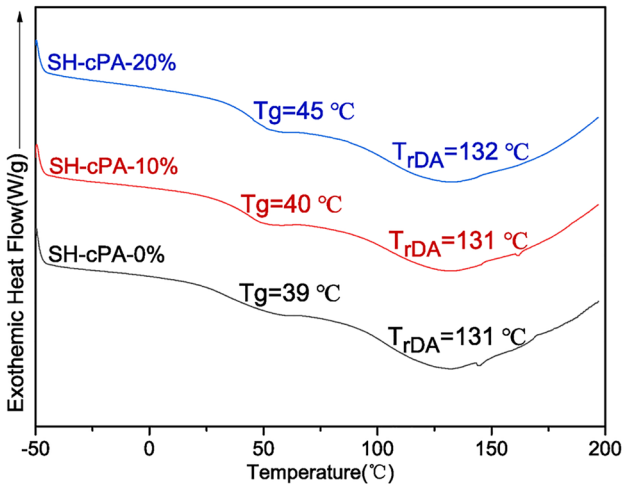

Fig. 7 DSC curves of SH-cPAs

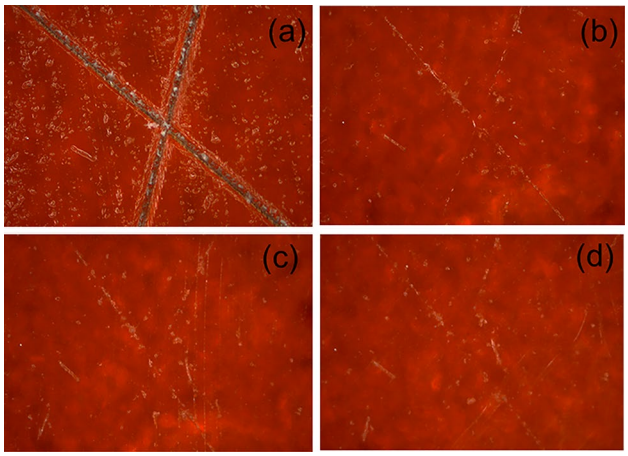

Fig. 8 Repairing process of SH-cPA-10% observed under a polarizing microscope (×64) (130 °C). (**a**) 0 h, (**b**) 30 min, (**c**) 1 h, (**d**) 1.5 h

and also confirm the successful DA reaction between pFU-PA-10% and BMIMP. In summary, SH-cPAs were successfully prepared from BMIMP and pFU-PAs.

DSC characterization

DSC characterization shows the thermal properties of SH-cPAs. In Fig. 7, no exothermic peaks were observed on the DSC curves, indicating that the DA reaction was complete when they were cured at 60 °C for 30 h. In addition, a clear endothermic peak was shown at around 131 or 132 °C, which corresponded to the reverse DA (rDA) reaction. DSC characterization confirms the DA bonds formed in SH-cPAs. The glass transition temperature (T_g) of SH-cPAs is between 39 and 45 °C (Table 2). As the content of MX-FU-DPA hard segmenets (HSs) increases, the T_g of SH-cPAs increases because MX-FU-DPA HSs contain rigid benzene rings. Although SH-cPA-0%, SH-cPA-10%, and SH-cPA-20% exhibied almost the same rDA temperature, DSC measurements clearly showed the difference of their T_gs. Low MX-FU-DPA HS content less than 20 mol% caused small difference in their thermal properties.

Swelling property of SH-cPAs

After soaked in DMF at 60 °C for 8 h, the dissolution ratio of SH-cPAs was detected. The dissolution ratio is lower than 10.84% (Table 2). SH-cPAs were crosslinked mostly, with small amount of linear or hyperbranched polyamides was left. Thus, small dissolution ratio was detected.

In order to further prove the high-temperature reversibility, SH-cPAs were soaked at 130 °C for 4 h. Then, all of them were completely dissolved in DMF. Figure S9 shows a typical example, i.e. SH-cPA-10%, after soaked at different temperatures. At 130 °C, the rDA temperature was reached. SH-cPAs underwent a de-crosslinking reaction and gradually decomposed into furan and maleimide groups. By swelling and dissolving them at different temperatures, we prove that SH-cPAs with reversible DA groups were synthesized.

Table 2 Properties of SH-cPAs

SH-cPAs	T_g (°C)	Dissolution ratio(%)	Tensile strength (MPa)		Strain at break (%)		Healing efficiency (%)
			Pristine	Healed	Pristine	Healed	
SH-cPA-0%	39	10.84	12	11	164	97	92
SH-cPA-10%	40	4.59	27	21	32	27	78
SH-cPA-20%	45	3.35	37	26	27	20	70

Self-healing properties of SH-cPAs

Figure S10 shows the cut-repair photos of SH-cPA-10%. A dumbbell spline was cut from the middle. The fracture was rejoined together and the cut edges were almost entirely repaired at 130 °C in 2 h. This experimental phenomenon indicates that SH-cPAs has good self-healing property.

Figure 8 shows the self-healing behavior observed with a dm2500p polarizing microscope. The surface of a SH-cPA-10% spline was scratched in cross directions with a knife. The scratches were repaired in a vacuum oven at 130 °C, and observed with POM every 30 min. The repairing was nearly complete at 30 min. At 1 h and 1.5 h, merely slight scratched signs were observed on the SH-cPA-10% spline.

Mechanical properties

The self-healing property of SH-cPAs was also characterized by the tensile test before and after healed. In Fig. 9 and Table 2, the original SH-cPAs exhibited tensile strength of 12–37 MPa and strain at break of 27%-164%. With the increase of MX-FU-DPA content, the tensile strength is significantly improved, while the strain at break or the toughness decreases. As the MX-FU-DPA segments are short and rigid HSs, increasing HS content increases the T_g and intermolecular interactions, but decreases the toughness. Thus, the tensile strength increases but the strain at break decreases. After repairing, SH-cPAs still showed tensile strength up to 26 MPa with repairing efficiency above 70%. SH-cPA-0% exhibited obviously better repair efficiency than SH-cPA-10% and SH-cPA-20%, because SH-cPA-0% contains merely flexible D230 soft segments (SSs). When SH-cPA-0% was damaged, its flexible chains moved more freely during the repair process. This flexible structure is conducive to the repair of cracks. With the increase of MX-FU-DPA content, the repair efficiency gradually decreases, maybe because the rigid and highly hydrogen-bonded HSs restricted the movement of molecular chains.

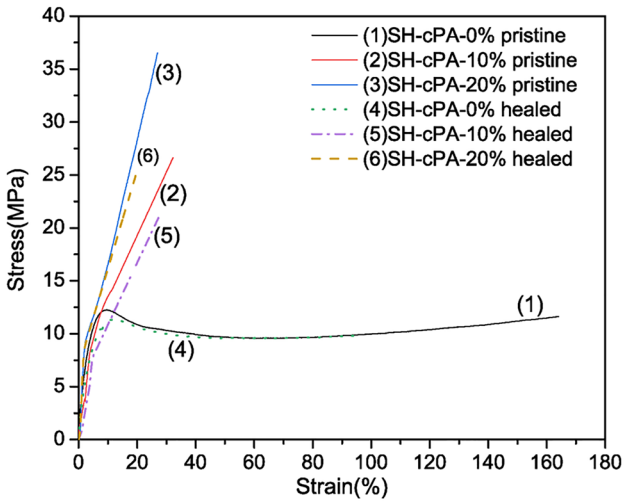

Fig. 9 Stress–strain curves of the pristine and healed SH-cPAs

Conclusions

Several self-healing crosslinked polyamides, i.e. SH-cPAs, were synthesized simply through a bulk Michael addition, polycondensation, and DA addition. SH-cPAs were constructed mainly with furfurylamine-N,N-dipropionamide (FU-DPA), m-xylylene, and polypropylene glycol or D230 segments. The properties of SH-cPAs were affected highly by *m*-xylylene and D230 contents. Increasing the *m*-xylylene content led to more stiff MX-FU-DPA HSs formed, which caused high T_g, strong intermolecular interactions, high tensile strength, and low flexibility or strain at break. D230 SSs bring good toughness to SH-cPAs. D230 content affects the repairing efficiency of SH-cPAs. SH-cPAs with high D230 content show high repairing efficiency. SH-cPAs exhibit T_g from 39 to 45 °C, tensile strength up to 37 MPa, and strain at break of 27%-164%. The thermally repaired SH-cPAs still show good tensile strength up to 26 MPa with the repairing efficiency of 70–92%. SH-cPAs can be easily prepared from common industrial starting materials. They may extend the application of cPAs and have wide promising uses in self-repairing coatings, adhesives, and composites.

Support information

Figures S1 and S2, the ^{1}H and ^{13}C NMR spectra (*d*6-DMSO) of BMIMP; Figs. S3 and S4, the ^{13}C NMR spectrum (*d*6-DMSO) and the related structure units of pFU-PA-10%; Figs. S5 and S6, the ^{1}H NMR spectrum (*d*6-DMSO) and the related structure units of SH-cPA-10%; Figs. S7 and S8, the ^{13}C NMR spectrum (*d*6-DMSO) and the related structure units of SH-cPA-10%; Fig. S9, the swelling-dissolution diagrams of SH-cPA-10%; Fig. S10, the cut-repair photos of SH-cPA-10% spline.

Supplementary information The online version contains supplementary material available at https://doi.org/10.1007/s10965-020-02404-x.

Acknowledgments This work was financially supported by Beijing Natural Science Foundation (No. 2182056).

References

1. Brewis DM, Comyn J, Cope BC, Moloney AC (1980) Effect of carriers on the performance of aluminium alloy joints bonded with an epoxide-polyamide adhesive. Polymer 21:344–351
2. Yin J, Zhu GC, Deng BL (2016) Graphene oxide (GO) enhanced polyamide (PA) thin-film nanocomposite (TFN) membrane for water purification. Desalination 379:93–101
3. Osswald T, Menges G (2003) Failure and damage of polymers. In: Osswald T, Menges G (ed) Materials Science of Polymers for Engineers. Hanser Publishers, Munich
4. Burattini S, Greenland BW, Chappell D, Colquhoun HM (2010) Healable polymeric materials: a tutorial review. Chem Soc Rev 39:1973–1985
5. Yang Y, Urban MW (2013) Self-healing polymeric materials. Chem Soc Rev 42:7446–7467
6. Yang J, Keller MW, Moore JS, White SR, Sottos NR (2008) Microencapsulation of isocyanates for self-healing polymers. Macromolecules 41:9650–9655
7. Wang W, Xu LK, Sun HY, Li XB, Zhao SH, Zhang WN (2015) Spatial resolution comparison of AC-SECM with SECM and their characterization of self-healing performance of hexamethylene diisocyanate trimer microcapsule coatings. J Mater Chem A Mater Energy Sus 3:5599–5607
8. Garcia SJ (2014) Effect of polymer architecture on the intrinsic self-healing character of polymers. Eur Polym J 53:118–125
9. Chen Y, Kushner AM, Williams GA, Guan Z (2012) Multiphase design of autonomic self-healing thermoplastic elastomers. Nat Chem 4:467–472
10. Jia XY, Mei JF, Lai JC, Li CH, You XZ (2015) A self-healing PDMS polymer with solvatochromic properties. Chem Comm (Cambridge, United Kingdom) 51:8928–8930
11. Kalista SJ, Ward TC (2007) Thermal characteristic of the self-healing response in poly(ethylene-co-methacrylic acid) copolymers. J R Soc Interface 4:405–411
12. Lee SH, Shin SR, Lee DS (2019) Self-healing of cross-linked PU via dual-dynamic covalent bonds of a Schiff base from cystine and vanillin. Mater Des 172:107774
13. Lei ZQ, Xiang HP, Yuan YJ, Rong MZ, Zhang MQ (2014) Room-temperature self-healable and remoldable cross-linked polymer based on the dynamic exchange of disulfide bonds. Chem Mater 26:2038–2046
14. Fan LF, Rong MZ, Zhang MQ, Chen XD (2018) Repeated intrinsic self-healing of wider cracks in polymer via dynamic reversible covalent bonding molecularly combined with a two-way shape memory effect. ACS Appl Mater Interfaces 10:38538–38546
15. Zhong YT, Wang XL, Zheng Z, Du PF (2015) Polyether–maleimide-based crosslinked self-healing polyurethane with Diels-Alder bonds. J Appl Polym Sci 132:41944
16. Yang L, Lu XL, Wang ZH, Xia HS (2018) Diels-Alder dynamic crosslinked polyurethane/polydopamine composites with NIR triggered self-healing function. Polym Chem 9:2166–2172
17. Turkenburg DH, Fischer HR (2015) Diels-Alder based, thermo-reversible cross-linked epoxies for use in self-healing composites. Polymer 79:187–194
18. Liu YL, Chuo TW (2013) Self-healing polymers based on thermally reversible Diels-Alder chemistry. Polym Chem 4:2194–2205
19. Tian Q, Rong MZ, Zhang MQ, Yuan YC (2010) Synthesis and characterization of epoxy with improved thermal remendability based on Diels-Alder reaction. Polym Intern 59:1339–1345
20. Du PF, Wu MY, Liu XX, Zheng Z, Wang XL, Joncheray T, Zhang YF (2014) Diels–Alder-based crosslinked self-healing polyurethane/urea from polymeric methylene diphenyl diisocyanate. J Appl Polym Sci 131:40234
21. Chen XX, Dam MA, Ono K, Mal A, Shen HB, Nutt SR, Sheran K, Wudl FA (2002) Thermally re-mendable cross-linked polymeric material. Science 295:1698–1702
22. Mcelhanon JR, Russick EM, Wheeler DR, Loy DA, Aubert JH (2002) Removable foams based on an epoxy resin incorporating reversible Diels-Alder adducts. J Appl Polym Sci 85:1496–1502
23. Liu YL, Hsieh CY, Chen YW (2006) Thermally reversible cross-linked polyamides and thermo-responsive gels by means of Diels-Alder reaction. Polymer 47:2581–2586
24. Kossmehl G, Nagel HI, Pah A (1995) Cross-linking reactions on polyamides by bis- and tris(ma1eimide)s. Angew Makromol Chem 221:139–157
25. Huang CQ, Luo SY, Xu SY, Zhao JB, Jiang SL, Yang WT (2010) Catalyzed chain extension of poly(butylene adipate) and poly(butylene succinate) with 2,2'-(1,4-phenylene)-bis(2-oxazoline). J Appl Polym Sci 115:1555–1565
26. Yi CF, Zhao JB, Zhang ZY, Zhang JY (2017) Cross-linked polyamides synthesized through a Michael addition reaction coupled with bulk polycondensation. Ind Eng Chem Res 56:13743–13750
27. Ban JL, Li SQ, Yi CF, Zhao JB, Zhang ZY, Zhang JY (2019) Amorphous and crystallizable thermoplastic polyureas synthesized through a one-pot non-isocyanate route. Chin J Polym Sci 37:43–51